Response of Polyatomic Molecules to Ultrastrong Laser- and Ion-Induced Fields

T. Schlathölter* and R. Hoekstra
KVI Atomic Physics, Rijksuniversiteit Groningen, Zernikelaan 25, 9747AA Groningen, The Netherlands

S. Zamith, Y. Ni, H. G. Muller, and M. J. J. Vrakking
FOM Institute for Atomic and Molecular Physics (AMOLF), Kruislaan 407, 1098SJ Amsterdam, The Netherlands
(Received 16 November 2004; published 13 June 2005)

The exposure of molecules to short, ultrastrong electric fields leads to multiple ionization and a subsequent Coulomb explosion. We present a comparative study where uracil molecules are exposed to fields generated by high-power laser pulses ($\tau \approx 75$ fs, $I > 10^{16}$ W/cm^2) or swift highly charged ions (0.5 MeV Xe^{25+}) representing a half-cycle pulse of less than 10 fs duration. Molecular dynamics and structural information contained in the fragmentation pathways can be assessed separately. Despite the similar field strengths large differences in fragment kinetic energies are found which are related to field shape and duration with the aid of molecular dynamics simulations.

DOI: 10.1103/PhysRevLett.94.233001 PACS numbers: 33.80.−b, 31.15.Qg, 33.15.Ta, 34.70.+e

When a polyatomic molecule is exposed to electric fields of a strength comparable to the intramolecular field that the valence electrons are subject to, several valence electrons are stripped off. The resulting multiply charged complex is inherently unstable and eventually breaks apart. Particularly for field durations comparable to typical molecular vibration times (t_m), an influence of the temporal evolution of the field amplitude on the molecular fragmentation dynamics is expected.

We want to address the question whether we can experimentally distinguish between immediate ionization followed by a Coulomb explosion and slower processes, where ionization and fragmentation occur simultaneously. In recent years high-power femtosecond (fs) lasers have been used to study the latter process. Immediate ionization on the other hand can be achieved by using fast highly charged ions (HCI) whose interaction time with a molecule can even be in the sub-fs regime.

Mathur recently performed a study comparing fs-laser and HCI induced ionization of benzene [1]. He studied the dependence of molecular fragmentation patterns on the temporal field properties for three cases: $\tau = 35$ ps laser pulses ($\tau \gg t_m$), $\tau = 100$ fs laser pulses ($\tau \approx t_m$) and 100 MeV Si^{3+} ions ($\tau \ll t_m$). Despite the wide range of field durations, qualitatively similar fragmentation patterns were observed. This was attributed to similarities in the spatial distributions of laser and ion-induced fields: The electric field induced by the laser, related to the intensity via $I = 1.33 \times 10^{-3}\, E^2$, varies as a function of the distance from the laser focus, where maximum intensity is reached. Each intensity interval occupies a certain volume in the laser-molecule interaction region sampled by the spectrometer. The experimental data averages over a wide range of electric fields strengths weighted by the respective volumes. In the ion case, averaging also occurs, but now over electric field strengths for collisions at different impact parameter b.

In this Letter, we focus on a comparative study of a $I \leq 5 \times 10^{16}$ W/cm^2 ($\tau \geq 75$ fs) laser pulse ($E \approx 5 \times 10^{16}$ W/cm^2) and a 0.5 MeV Xe^{25+} ($E \approx 5 \times 10^{16}$ W/cm^2 at $b \approx 3$ Å) induced Coulomb explosion of the RNA base uracil ($C_4H_4N_2O_2$), a six-membered ring (see Fig. 1). The different constituent atoms of uracil allow its dissociation to be investigated in far more detail than benzene. Similar to benzene [1], we observe uracil fragmentation patterns that are barely dependent on the ionization mechanism (see Fig. 1). However, striking differences in the fragment ion kinetic energies are evident. The experimental data is interpreted with the help of molecular dynamics calculations. We will show that the energies obtained from the HCI experiments can be used as a reference for interpreting the fs-laser data.

For fs-laser pulses, at intensities of the order of 10^{13} W/cm^2 the electric field induced distortion of the molecular potential allows electrons to pass over the Coulomb barrier. A transition from multiphoton ionization

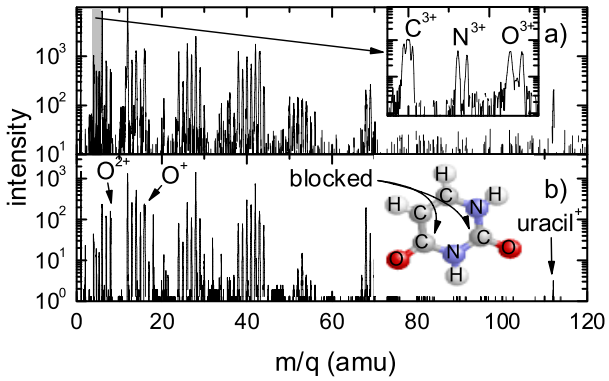

FIG. 1 (color online). Mass spectra of uracil fragment cations induced by Xe^{25+} ions [0.5 MeV, (a)] and laser pulses [$\tau \approx 75$ fs, $I \leq 5 \times 10^{16}$ W/cm^2, polarization parallel to the detection axis, (b)].

to field ionization occurs at a field strength that depends on the molecular geometry and composition [2]. For fs pulses at 10^{13}–10^{14} W/cm^2 interacting with polyatomic molecules, single ionization is the dominant channel and fragmentation remains moderate [2,3]. Multiple ionization is observed for intensities exceeding 10^{14} W/cm^2 and above 10^{16} W/cm^2 the Coulomb explosion into multiply charged fragments dominates [4]. Benzene has been the subject of several fs-laser induced ionization and fragmentation studies targeted at polyatomic molecules. At 10^{17} W/cm^2 Shimizu *et al.* [5] found the Coulomb explosion to take place at expansions of the molecular skeleton much smaller than expected from experiments on diatomics, where a doubling of the internuclear distances occurs [6–8]. However, Tzallas *et al.* did find this doubling for a variety of aromatic molecules at 4×10^{16} W/cm^2 [9] and a strong dependence of the dissociation process on the molecules aromaticity [10].

A HCI can be viewed as a point charge passing the molecule. Depending on the impact parameter and charge state, such a ''half-cycle'' pulse can have a magnitude and duration similar to the field of a fs-laser pulse of several optical cycles. The multiple ionization is similarly described in terms of electron transfer over the barrier between the Coulomb potentials of the molecule and the HCI [11]. In the context of HCI collision studies, polyatomic molecules are of interest as intermediates, lying between van-der-Waals clusters with loosely bound and weakly interacting constituents [12] and the strongly bound, almost metallic fullerenes [13].

Our laser experiments were performed at AMOLF using a 50 Hz Ti:Sa laser. For the HCI experiments, the KVI 14 GHz electron cyclotron resonance ion source, floated on a potential of 20 kV, was employed. After magnetic mass-selection, the continuous ion beam was collimated to 1 mm. Both the laser and the HCI beams were focussed into the extraction region to interact with a gaseous uracil target evaporated from an oven that was heated to 180 °C to ensure maximum target density without thermal fragmentation. Using base pressures below 3×10^{-8} mbar, residual gas contributions were negligible. Charged particles were extracted from the collision region by means of a moderate static electric field (for most experiments 300 V/cm) between two surrounding electrodes. The cations were focussed into a reflectron time-of-flight (TOF) spectrometer (resolution $\frac{\Delta m}{m} = 1/1500$ at $m = 720$ amu [14]). For masses up to the uracil parent ion ($m =$ 112 amu) the detection efficiency varies by less than 0.5% [14]. For the laser experiment, TOF signals triggered by a photodiode signal were fed into a HP Infinium digital storage oscilloscope and averaged over 1000 sweeps. In the Xe^{25+} HCI experiments an electron from an ionization event started a multihit FAST P7888 time-to-digital converter and several fragment ions were recorded in coincidence [15].

Figure 1 illustrates the similarity in fragmentation patterns produced by fs-laser pulses and a HCI where H^+, C^{q+}, N^{q+} and O^{q+} ions are formed with very similar abundances. The fragment ion peaks (Fig. 1, zoom of the region marked in gray) exhibit a double structure with a time separation Δt due to fragments emitted towards the detector (short TOF) and in the opposite direction (long TOF), that allows extraction of the fragment energies. For a given extraction field ε, fragment charge state q and ion mass m the fragment ion kinetic energy is given by $E = \varepsilon^2 q^2 \Delta t^2 / 8m$. Kinetic energy distributions for C^{q+}, N^{q+} and O^{q+} ($q = 1$–3) are displayed in Fig. 2. The spectra are not corrected for transmission effects induced by the extraction diaphragm.

For all fragment ion species a qualitatively similar behavior is observed in the laser and in the HCI case: For singly charged ions the kinetic energy peaks at about 0 eV. The peak energy increases with the fragment ion charge state. Only for $C^{2+/3+}$ the energy distributions still have a strong contribution at 0 eV. These low-energy ions originate from ''blocked'' sites (see Fig. 1) [15]. The light H atoms have no such ''blocking'' effect and do not hinder the movement of their neighbors. O^{q+} ions, originating from outside the ring, experience the remaining molecule as a point charge and exhibit highest kinetic energies. N^{q+} ions from the ring have the lowest kinetic energies. Here, Coulomb repulsion from the neighbors partially cancels.

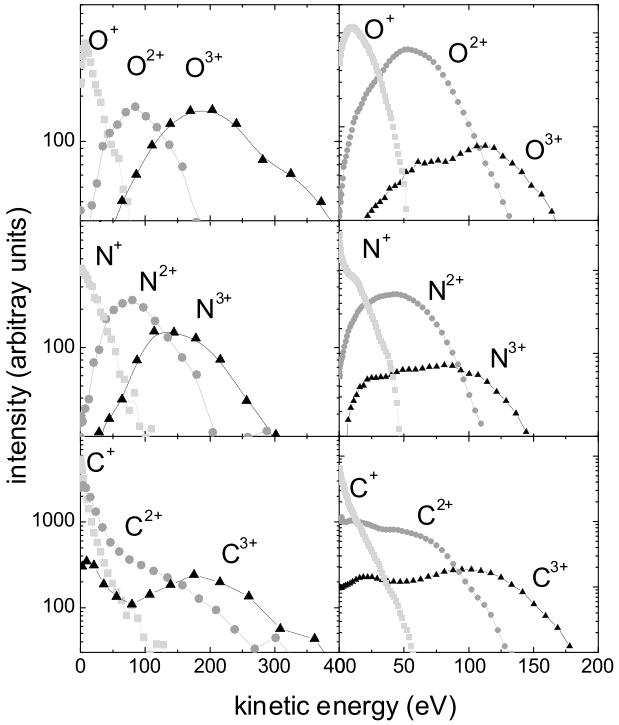

FIG. 2. Kinetic energy distributions for O^{q+} (top), N^{q+} (middle) and C^{q+} (bottom). Left: interaction with 0.5 MeV Xe^{25+}, right: laser ($\tau \approx 75$ fs, $I \leq 5 \times 10^{16}$ W/cm^2).

Despite the similar trends in fragment energies for laser and HCI induced fragmentation, the quantitative differences are dramatic. In the HCI case the fragment energies are larger by about a factor of 2. The maximum energies for C^{3+} and O^{3+} are ≈ 175 eV in the laser experiment (with only weak dependence on the laser peak intensity) but 350–400 eV for HCI impact. Typical molecular vibration times are of the order of 3×10^{-14} to 10^{-12} s which is long compared to the ion and laser induced ionization. However, multiple ionization drives fragmentation much faster. In the fs-laser case, it sets in *during* the pulse. The molecular skeleton expands from onset of ionization and highest fragment charge states are formed at increased intramolecular distances. A Coulomb explosion at enlarged bond-lengths has been observed for small [6–8] as well as for polyatomic molecules [9,10]. Even alignment along the laser polarization axis as well as molecular deformation during the pulse have been found [16–18].

The half-cycle nature of the HCI impact on the other hand, leads to a much shorter interaction of typically much less than 10 fs. On such short timescales, even the skeleton of a multiply charged molecular complex stays essentially frozen. The HCI results in Fig. 2 thus reflect Franck-Condon type multiple ionization, whereas the fs-laser results arise from a convolution of ionization and fragmentation due to the multicycle ionization dynamics in the laser field.

So far, the interpretation of fs-laser induced fragmentation by means of molecular dynamics simulation has started by considering (symmetric) model charge distributions within the intact molecule [5,9], and performing calculations including the laser field and sometimes the electron dynamics in the simulation [19]. Our half-cycle approach using HCI, however, provides experimental data for a Coulomb explosion of a molecule from its equilibrium geometry which can be used directly as a reference.

Table I summarizes the peak positions and the maximum kinetic energies obtained from Fig. 2 for the laser and the HCI case. As in [19] $E_{\max}$ is defined as the energy where the energy distribution drops to 20% of its maximum. For multiple peaks (C^{q+}) only the highest energy peak is given.

TABLE I. Peak positions and maximum kinetic energies (in eV) from Fig. 2.

ion	$E^{\text{ion}}_{\text{peak}}$	$E^{\text{ion}}_{\max}$	$E^{\text{laser}}_{\text{peak}}$	$E^{\text{laser}}_{\max}$	$E^{\text{laser}}_{\max}/E^{\text{ion}}_{\max}$
O^{1+}	7.3	56	10	46	82%
O^{2+}	85	175	53	97	55%
O^{3+}	187	383	111	162	42%
N^{1+}	0	55	11	31	56%
N^{2+}	77	182	42	86	47%
N^{3+}	144	280	79	141	50%
C^{1+}	0	15	0	11	73%
C^{2+}	85	214	44	95	44%
C^{3+}	176	335	97	160	48%

For N^{q+} ions the maximum kinetic energies in the laser case $E^{\text{laser}}_{\max}$ are similar to the benzene data (C^{q+} peaks) from [19] obtained with comparable laser parameters (8×10^{16} W/cm^2, $\tau = 120$ fs). O^{q+} located outside the ring has generally higher energies. Surprisingly, C^{q+} originating partly from "open" sites has almost the same kinetic energy distribution as O^{q+}.

The last column of Table I compares $E_{\max}$ values from Franck-Condon type ionization induced by the HCI half-cycle pulses with those from laser ionization. For fragment charge states 2+ and 3 + , the kinetic energies in the HCI case are twice as high as for the laser case.

To understand whether the energy difference between the laser and HCI induced ionization is purely due to the different pulse durations, we performed molecular dynamics simulations. Only interactions among charged particles are taken into account as mediated by a soft-core Coulomb potential $V(r_{ij}) = 1/(r_{ij}^2 + a_i + a_j)^{0.5}$ with a_i and a_j chosen such that an electron j is subject to the atomic ionization potential of atom i when located at $r_{ij} = 0$. For each run, 12 neutral atoms at rest are initialized to their respective equilibrium coordinates [20], with a randomly oriented molecule. The time-dependent external dipole field of the laser along its polarization axis is defined as $V_{\text{laser}}(t) = E_0 \sin(2\pi t/T)\sin^2(\pi t/\tau)$ with the laser period T and the total pulse length τ. The intensity is randomly chosen within a Gaussian beam profile and tunnel ionization is treated according to the Ammosov-Delone-Krainov (ADK) model [21]. Electron impact ionization (recollisions) is accounted for with a rate determined by Lotz's cross section [22]. In the HCI case the field is that of a moving point charge, with impact parameter b randomly chosen for each trajectory.

Each atom consists of an ion neutralized by an electron placed in the center of the respective soft-core Coulomb potential. This is done to prevent tunnel ionization from occurring without external fields. At typical internuclear distances in the molecule a singly ionized atom would tunnel ionize its neighbors, thus initiating an avalanche. After the external field removed the outermost electron, the remaining ion can be tunnel ionized further. As soon as such a tunnel-ionization event takes place the charge state of the respective atom/ion is incremented by one. An electron is set free and becomes a separate particle. The whole system is propagated in time by solving Newton's equations numerically. Molecular properties are neglected. In reality the first electrons are removed from an intact molecule where the charges are still mobile and where the ionization potential differs from those of the single atoms. Furthermore, Bhardwaj *et al.* [23] showed recently that cluster and molecule ionization and fragmentation by strong fields can be strongly influenced by laser induced intramolecular dipole forces. Molecular effects are of importance in the initial phase of the interaction. Because of their neglect, the simulation yields fragment kinetic ener-

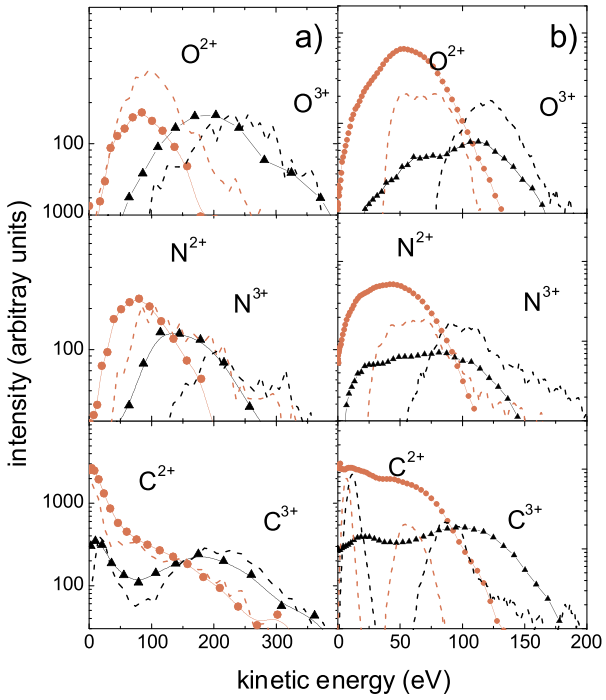

FIG. 3 (color online). Kinetic energy distributions for O^{q+} (top), N^{q+} (middle) and C^{q+} (bottom). Symbols: experiment, data from Fig. 2. dashed: simulation. (a) 0.5 MeV Xe^{25+}, (b) laser ($\tau = 150$ fs, $I = 3.5 \times 10^{16}$ W/cm^2).

gies that are too high for the singly charged fragments. Agreement of experiment and simulation is expected for multiply charged fragments which originate from a intermediate complex whose molecular nature had already disappeared.

The solid curves with symbols in Fig. 3 represent the experimental data from Fig. 2 and the dashed lines are the simulation results. Indeed, for the HCI case energies about twice as high as for the laser are found. A pulse length $\tau = 150$ fs in the simulation yielded optimum agreement with the experimental results. The simulation slightly overestimates the kinetic energies for O^{q+} (HCI and laser) as well as N^{3+} (HCI), but qualitative agreement with the experiment is obtained. Highest peak kinetic energies are observed for the O^{q+} ions, N^{q+} ions peak at lower energy and C^{q+} ions exhibit a double peak structure. C^{q+} ions from blocked sites (see Fig. 1) peak at energies close to zero, whereas the ions from open sites have kinetic energies similar to those of O^{q+} ions. The double peak structure is particularly well reproduced in the simulation. In the laser case, the experimental peak widths are broader than the simulations due to the limited resolution of the spectrometer. Furthermore, for the laser as well as the HCI case, transmission effects favor the low-energy contribution in the experimental data.

In conclusion, we have compared the response of neutral uracil molecules upon the strong perturbation by 75 fs-laser pulses and half-cycle pulses due to passage of 0.5 MeV Xe^{25+} ions. A similar overall fragmentation pattern for laser and ion-induced fragmentation has been observed, in line with the results of Mathur [1]. In the HCI case, multiple ionization takes place on the time scale of several fs where the motion of the nuclei is essentially frozen, whereas for the laser, ionization and fragmentation time scales are similar. The multiply charged fragment energies differ by a factor of 2 from the laser to the HCI case, as confirmed by our simulations. In both cases the fragment energies reflect the molecular geometry. Fragment ion kinetic energies from HCI induced Coulomb explosion might serve as a reference for similar fs-laser studies, where ionization is a multistep process accompanied by strong motion of the nuclei.

We gratefully acknowledge financial support from the Stichting voor Fundamenteel Onderzoek der Materie (FOM) which is supported by the Nederlandse Organisatie voor Wetenschapelijk Onderzoek (NWO). T. S. acknowledges support by the Royal Netherlands Academy of Arts and Sciences. S. Z. acknowledges financial support from the Marie Curie programme of the EC.

*Electronic address: tschlat@kvi.nl

[1] D. Mathur, Phys. Rev. A **63**, 032502 (2001).
[2] R. J. Levis and M. J. DeWitt, J. Phys. Chem. A **103**, 6493 (1999).
[3] A. Talebpour *et al.*, J. Phys. B **33**, 4615 (2000).
[4] D. J. Smith *et al.*, Rapid Commun. Mass Spectrom. **13**, 1366 (1999).
[5] S. Shimizu *et al.*, Chem. Phys. Lett. **317**, 609 (2000).
[6] J. H. Posthumus *et al.*, J. Phys. B **28**, L349 (1995).
[7] J. H. Posthumus *et al.*, J. Phys. B **29**, 5811 (1996).
[8] E. Constant, H. Stapelfeldt, and P. B. Corkum, Phys. Rev. Lett. **76**, 4140 (1996).
[9] P. Tzallas *et al.*, Chem. Phys. Lett. **332**, 236 (2000).
[10] P. Tzallas *et al.*, Chem. Phys. Lett. **343**, 91 (2001).
[11] A. Niehaus, J. Phys. B **19**, 2925 (1986).
[12] W. Tappe *et al.*, Phys. Rev. Lett. **88**, 143401 (2002).
[13] S. Martin *et al.*, Phys. Rev. A **66**, 063201 (2002).
[14] O. Hadjar *et al.*, Phys. Rev. A **63**, 033201 (2001).
[15] J. de Vries *et al.*, Phys. Rev. Lett. **91**, 053401 (2003).
[16] J. H. Sanderson *et al.*, Phys. Rev. A **59**, R2567 (1999).
[17] W. A. Bryan *et al.*, J. Phys. B **33**, 745 (2000).
[18] F. Rosca-Pruna *et al.*, J. Phys. B **34**, 4919 (2001).
[19] S. Shimizu *et al.*, J. Chem. Phys. **117**, 3180 (2002).
[20] M. K. Shukla and P. C. Mishra, Chem. Phys. **240**, 319 (1999).
[21] M. V. Ammosov, N. B. Delone, and V. P. Krainov, Sov. Phys. JETP **64**, 1191 (1986).
[22] W. Lotz, Z. Phys. **216**, 241 (1968).
[23] V. R. Bhardwaj, P. B. Corkum, and D. M. Rayner, Phys. Rev. Lett. **91**, 203004 (2003).